Effects of Grafting Density and Molecular Weight on the Temperature-Dependent Conformational Change of Poly(*N*-isopropylacrylamide) Grafted Chains in Water

H. Yim and M. S. Kent*

Department 8332, Sandia National Laboratories, Albuquerque, New Mexico 87185

S. Mendez and G. P. Lopez

Department of Chemical and Nuclear Engineering, University of New Mexico, Albuquerque, New Mexico 87131

S. Satija and Y. Seo

National Institute of Standards and Technology, Gaithersburg, Maryland 20899

Received September 27, 2005; Revised Manuscript Received February 16, 2006

ABSTRACT: Poly(*N*-isopropylacrylamide) (PNIPAM) is perhaps the most well-known member of the class of responsive polymers. Free PNIPAM chains have a lower critical solution temperature (LCST) in water at about 30 °C. This very sharp transition (about 5 °C) is attributed to alterations in the hydrogen-bonding interactions of the amide groups. Grafted chains of PNIPAM have shown promise for creating responsive surfaces. Conformational changes of the polymer are likely to play a role in some of these applications, in addition to changes in local interactions. In this work we investigated the temperature-dependent conformational changes of grafted PNIPAM chains in D_2O over a range of surface density and molecular weight using neutron reflection. The surface density was controlled using mixed self-assembled monolayers. The molecular weight was controlled using atom transfer radical polymerization (ATRP). Grafted layers were synthesized on gold and also on silicon oxide. The largest conformational changes were observed for intermediate grafting densities and high molecular weights. This is explained by a competition between the well-known chain stretching effect of laterally interacting tethered chains and the phenomenological $\chi(\phi)$ determined empirically for PNIPAM free chains in water. Comparison is made with the recent numerical SCF calculations of Mendez et al.

Introduction

Poly(*N*-isopropylacrylamide) (PNIPAM) exhibits a lower critical solution temperature (LCST) of ∼30 °C in water that is attributed to a shift in the distribution of the hydrophobic and hydrogen-bonding interactions.[1−4] Grafting PNIPAM to surfaces is a promising strategy for creating responsive surfaces, since the physical properties of PNIPAM are readily altered by changing the temperature. PNIPAM in various forms has been explored for a variety of applications.[5−13] Some of these applications depend primarily upon the shift in short-ranged interactions, such as controlling the adsorption of bacteria[13] and tissue cells[10,12] through changes in hydrophobicity. However, some applications depend critically upon the magnitude of the conformational changes that result from the shift in fundamental interactions, such as separating molecules on the basis of size[7,8] and controlling ligand binding to receptors.[6] For applications such as these, it is important to understand how to maximize the conformational change.

Brushes formed of polymers tethered by one end to a surface or an interface have been examined in great detail over the past 2 decades.[14−18] Most of this work involved UCST systems governed by van der Waals interactions. For such systems, the effects of the surface density (σ) and molecular weight (M) on brush properties have been examined in detail both theoretically and experimentally. The distinctive feature is that for sufficiently high σ that the chains overlap laterally the osmotic interaction causes the chains to stretch normal to the surface until the osmotic free energy is balanced by the entropic elastic free energy. In the scaling limit, achieved for high values of reduced surface density $\sigma\pi R_g^2$, the brush height h varies as $h \sim M\sigma^{1/3}$.

The case of hydrogen-bonding polymers in water is more complex. In addition to the effect of surface density on chain crowding and subsequent stretching, an additional dependence on surface density arises for polymers that have an LCST such as poly(ethylene oxide) (PEO) and PNIPAM from the concentration dependence of the effective Flory χ parameter. For PNIPAM this dependence was obtained recently in a study of the phase behavior of free chains in solution.[19] For hydrogen-bonding polymers in water, the concentration dependence of the effective Flory χ parameter has been explained in terms of various two state models, in which the monomers interconvert between two states depending upon the local concentration.[20−24] The effects of this phenomenon on the structure and properties of polymer brushes have been addressed in a number of theoretical studies[25−34] and also through simulations.[35] The Karlstrom model was used in numerical self-consistent-field (SCF) calculations of the Scheutjens−Fleer type to describe the aggregation behavior of PEO−PPO−PEO block copolymers in water.[27−29] The *n*-cluster model was used to calculate brush structure using SCF theory[26] and to calculate force profiles upon compression of polymer brushes.[30,31] A recent theoretical analysis by Baulin and Halperin[32] identified the surface density as a critical parameter demarcating different regimes of behavior, focusing on the existence of a vertical phase separation within the brush at high surface density that had been proposed in previous analyses.[26,35] They examined vertical phase separation within PNIPAM brushes using a microscopic model based on

10.1021/ma0520949 CCC: $33.50
Published on Web 04/08/2006

the Pincus approximation.[32] This was followed by an analysis based on an analytical SCF theory.[33] More recently, Mendez et al. studied the temperature-induced structural changes of PNIPAM brushes as a function of M and σ with a numerical SCF.[34] They found that the change in thickness of the layer from 20 to 40 °C is a nonmonotonic function of surface density with a maximum that shifts to lower surface density as the chain length increases. Temperature-induced conformational changes in PNIPAM brushes have been studied by surface plasmon resonance,[36] atomic force microscopy (AFM),[37,38] and hydrodynamic radius measurements.[39−41] However, while much experimental work has been reported regarding the M and σ dependence of polymer brushes for UCST systems,[18,42] little data of that nature exist for LCST systems.[43]

We have been studying the temperature-dependent conformational changes of PNIPAM grafted chains in water as a function of surface density and molecular weight using neutron reflection (NR). In our first report[44] we investigated the conformational changes of PNIPAM chains tethered at low density to silicon oxide. The surface density ranged from 1×10^{-4} to 2×10^{-4} chains/Å^2. For these low surface density brushes, the conformational changes in D_2O were very subtle. No coil-to-globule transition was observed. This contrasted with a number of previous reports involving PNIPAM grafted layers in which various effects were interpreted in terms of large conformational changes.[4,12,45,46]

More recently, we reported the effect of M on the conformational change of PNIPAM chains grafted at high σ (5.4×10^{-3} chains/Å^2).[47−49] Samples with different M were grafted at the same high surface density onto gold-coated silicon by atom transfer radical polymerization (ATRP). A significant change in the segment concentration profile was observed for all three samples as the temperature passed through the LCST. Surprisingly, the fractional change in the first moment of the segment concentration profile ($\langle z \rangle$) from 20 to 41 °C was weaker with increasing M. This result is contrary to the trend for good and poor solvent conditions reported previously for systems involving only van der Waals (VDW) interactions.[18] The trend correlated with the bilayer character of the profile which also increased at lower M and will be discussed further below.

The present work emphasizes a range of σ intermediate to those in our previous reports. We find that the effect of M is particularly strong in this intermediate range of σ and that the magnitude of the conformational change with temperature at high M is much greater than observed for samples with comparable M at lower or higher σ. Samples with controlled M were synthesized by ATRP from gold-coated silicon wafers and also directly from silicon wafers. Surface density was controlled using mixed self-assembled monolayers (SAMs). Synthesis of PNIPAM from silicon oxide avoids the gold and chromium sputtering steps and also simplifies the data analysis. However, the packing density of the SAMs appears to be higher on gold. We report the data below and compare the results with the theoretical calculations of Mendez and co-workers.[34]

Experimental Section

Materials. 1-Dodecanethiol (DT), 11-mercapto-1-undecanol (MU), 2-bromopropionyl bromide, 2-bromoisobutyryl bromide, ethyl 2-bromoisobutyrate, CuBr, PMDETA (*N*,*N*,*N*′,*N*′,*N*″-pentamethyldiethylenetriamine), Me4cyclam (1,4,8,11-tetramethyl-1,4,8,11-tetraazacyclotetradecane), *N*-isopropylacrylamide (NIPAM), D_2O (99.9 atom %), anhydrous dimethylformamide (DMF), and anhydrous tetrahydrofuran (THF) were purchased from Aldrich Chemical Co.[50] Undecyltricholorsilane (UTS) was purchased from Gelest. NIPAM was recrystallized from hexane; all other materials were used as received.

Grafting PNIPAM from Gold. The detailed procedure for synthesis of PNIPAM on gold is described elsewhere.[36] Thin layers of chromium (30 Å) and gold (110 Å) were sequentially sputtered onto silicon wafers. The gold-coated wafers were cleaned by placing them into a UV/ozone cleaner for 20 min and were then submerged overnight in an ethanol solution containing a mixture of 1-dodecanethiol and 11-mercapto-1-undecanol. The composition was adjusted to control the grafting density. After an ethanol rinse, the monolayers were treated with 2-bromopropionyl bromide (0.1 M) in the presence of triethylamine (0.12 M) for 2−3 min to convert to a bromo-terminated ester. The initiator-modified samples were placed into a DMF solution containing the NIPAM monomer and CuBr/Me4cyclam catalyst (0.2 M) and allowed to react for various periods of time to obtain different M values. The reaction was carried out in a Vacuum Atmospheres glovebox purged with nitrogen. The samples were rinsed with DMF and ethanol to terminate the reaction and then cleaned with deionized water and methanol to remove unbound polymer.

Grafting PNIPAM from Silicon Oxide. To graft PNIPAM brushes directly from silicon oxide, an organosilane containing 2-bromo isobutyrate was used as the ATRP initiator. The synthetic procedure for the initiator (11-(2-bromo-2-methylpropinonyloxy)-undecyltrichlorosilane) is described in detail elsewhere.[51] The silicon wafers were cleaned with piranha solution and rinsed with water, followed by drying in a stream of nitrogen. The cleaned wafers were placed in a toluene solution containing a mixture of undecyltrichlorosilane and initiator, and the container was heated at 60 °C for 4 h. The silicon wafers were then removed, washed with toluene and ethanol, and then dried in a stream of nitrogen. The initiator-modified samples were then placed into an aqueous solution containing NIPAM monomer and CuBr/PMDETA and allowed to react for various periods of time.[52] The reaction was carried out in a glovebox purged with dry nitrogen gas. The samples were rinsed with THF to terminate the reaction and then cleaned with deionized water and methanol to remove unbound polymer.

Characterization of M and σ. To determine M for a particular sample, free PNIPAM was polymerized in solution simultaneous with a surface polymerization by addition of 0.4 mM methyl 2-bromoisobutyrate into the solution. Gel permeation chromatograhy (GPC) analysis was performed at Polymer Source (Canada) using polystyrene standards for calibration to obtain the weight-average molecular weights and polydispersities of the bulk polymerized material. DMF with 0.01 M LiBr (flow rate of 1 mL/min) was used as eluent. Polydispersities were 2.1 ± 0.2. The use of polystyrene standards for calibration is believed to lead to values that are ~15% higher than actual.[53] The weight-average molecular weight for the surface polymerized sample was assumed to be the same as that for the sample polymerized in bulk and measured by GPC. Several studies in the literature in which both surface and bulk polymerized samples were measured independently report that the values are within 20%.[54−57] Combining the uncertainties, we expect that our reported M values are accurate to within 25%. To calculate the surface density, the dry film thickness and density of each sample were measured by X-ray or neutron reflectivity. The surface density was then calculated using the molecular weight obtained by GPC for the corresponding bulk polymerized sample. The uncertainty in surface density is estimated to be ±25% as well. We assumed that the surface density was constant for all polymerizations with the same surface concentration of initiator. The characteristics of all samples are given in Table 1.

Instrumentation. The neutron reflectivity (NR) measurements were performed on the NG7 reflectometer at the National Institute of Standards and Technology (Gaithersburg, MD) at a fixed wavelength of 4.75 Å. Reflectivity data from the protonated PNIPAM layers in deuterated water were obtained using a liquid cell over a range of temperature from 10 to 41 °C. Neutron reflectivity probes the scattering length density (SLD) profile normal to the surface, which is determined by the density and atomic composition. The SLD profiles were converted to volume fraction profiles assuming additivity of volumes. The SLD profiles were composed of a stack of slabs, where each slab was assigned an

Table 1. Molecular Weights and Grafting Densities of PNIPAM Samples

sample	substrate	mol wt, g/mol	grafting density, chains/Å^2
33G	gold	33 000	0.00063
152G	gold	152 000	0.00063
76S	silicon	75 600	0.0021
230S	silicon	230 000	0.0008
52S	silicon	52 000	0.0008
71G[a,c]	gold	71 000	0.0054
44G[a]	gold	44 000	0.0054
13G[a]	gold	13 000	0.0054
33S[b]	silicon	33 000	0.00018
220S[b]	silicon	220 000	0.0001
209S[c]	silicon	209 000	0.0021

[a] Samples reported in ref 48. [b] Samples reported in ref 44. [c] Samples reported in ref 61.

SLD, a thickness, and a roughness. The data were analyzed using a small number of unconstrained layers (one or two) to represent the grafted PNIPAM profile. The reflectivity was calculated from the stack of slabs using the optical matrix method.[58] Best-fit profiles were determined by minimization of least squares. To constrain the fits to the NR data for the samples grafted to gold, the thicknesses and SLD values of the Cr, Au, silicon oxide, SAM, and dry PNIPAM films were determined in separate experiments. For the samples grafted to silicon oxide, the fits were constrained by determining the thickness and SLD of the silicon oxide, SAM, and dry PNIPAM films in separate experiments. X-ray reflectivity (XR), which determines the electron density profile normal to the surface,[59] was performed at Sandia National Labs using an instrument described previously[60] and at the National Institute of Standards and Technology using a reflectometer from Bruker with a Gobel mirror to monochromate the beam and slits both before and after the sample.

Results

NR data for 152G for a sequence of decreasing temperatures after heating above the LCST are shown in Figure 1a. The data are displayed as reflectivity $\times$ q^4 to compensate for the q^{-4} decay due to the Fresnel law. The data are shifted on the *y*-axis for clarity. The reflectivity returned to that of the original curve measured prior to heating (not shown) as the temperature was lowered back to 20 °C. The best-fit profiles are shown in Figure 1b. The profiles show that the PNIPAM chains expand significantly upon cooling from 41 to 20 °C. Regarding the profile shape, good agreement with the data requires a bilayer function in which a thin layer of higher density is included near the substrate. This may suggest some segmental adsorption. The segment volume fraction at the substrate surface at 20 °C is much lower for 152G (prepared using a solution with a 20/80 ratio by volume of MU to DT) than for our previous samples synthesized on gold (prepared using a solution containing a 90/10 ratio by volume of MU to DT), consistent with the expectation of a much lower surface density for 152G. We note that the variation in the profile shape with temperature is continuous through the transition. This finding is contrary to the results for high-*M* PNIPAM samples at high grafting density, where the change in profile shape near the transition temperature is nonmonotonic.[61]

Upon cooling, most of the conformational change occurred between 32 and 27 °C, as shown by the variation in the first moment in Figure 2. The first moment of the segment concentration profile increased from 100 to 400 Å with decreasing temperature. This is the largest change of layer thickness with *T* for any of our samples and is in contrast to our previous studies, in which much more modest changes in layer thickness were observed for PNIPAM chains at substantially higher or lower grafting densities. The surface density of 152G is 0.000 63 chains/Å^2, which is an order of magnitude

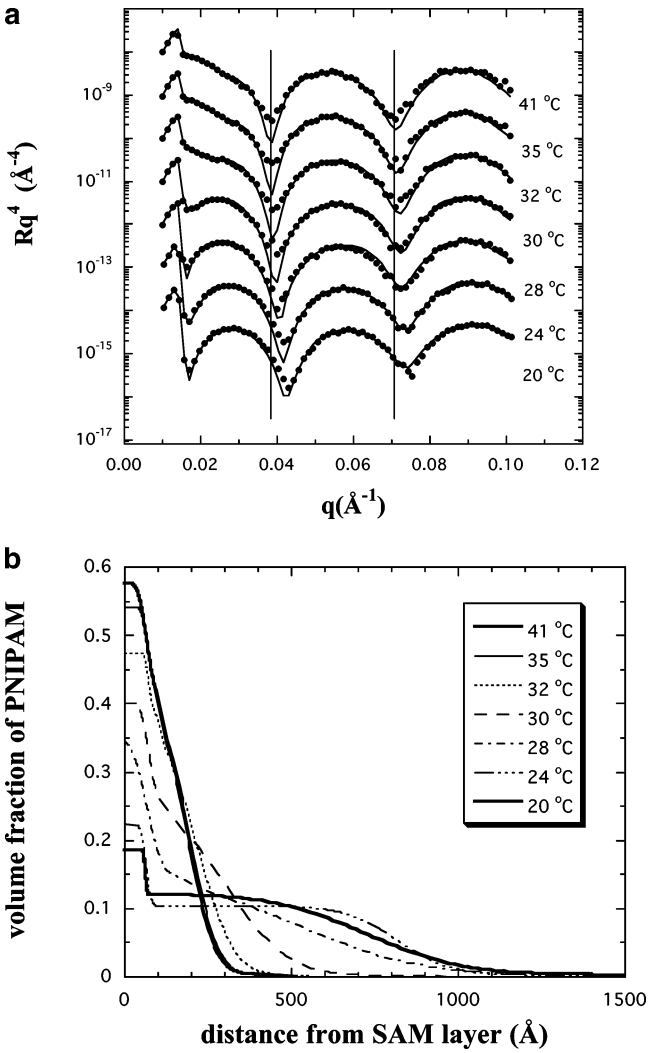

Figure 1. (a) Neutron reflectivity data from 152G for a series of temperatures beginning at 41 °C and cooling to 20 °C in D_2O. The curves through the data correspond to best fits using model segment concentration profiles shown in (b). (b) Best-fit concentration profiles.

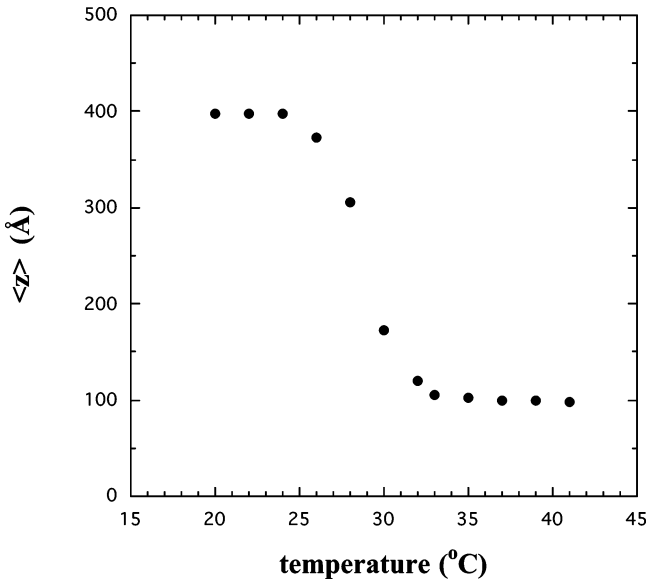

Figure 2. Variation of the first moment of the segment concentration profile with temperature upon cooling from 41 °C for 152G.

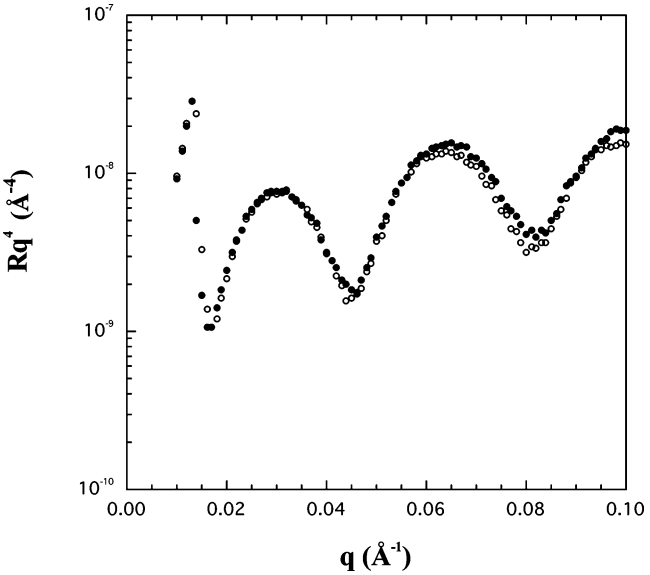

Figure 3. Neutron reflectivity data from 33G at 20 (open circle) and 41 °C (closed circle) in D_2O.

lower than that for the PNIPAM samples in one previous study[48] and a factor of 6 greater than that for a comparable molecular weight in another previous study.[44] This comparison clearly demonstrates that surface density is an important parameter that affects the magnitude of the change in PNIPAM conformation with temperature.

Figure 3 shows NR data for 33G at 20 and 41 °C. This PNIPAM layer was grown from a monolayer deposited from a solution with a 20/80 ratio by volume of MU to DT as for 152G. The lower molecular weight was achieved by allowing the polymerization to proceed for a shorter period of time. Unlike 152G, no change in reflectivity was observed over this temperature range. This result demonstrates that the temperature-dependent conformational change is a strong function of molecular weight for this intermediate σ.

Figure 4a shows NR data for 230S upon heating from 20 to 39 °C. For this sample, the PNIPAM chains were grafted using a solution with a 8/92 ratio by volume of initiator to UTS. The grafting density for this sample was 0.0008 chains/Å^2, much lower than that for 76S and 209S, which were grafted from a surface prepared with a solution of initiator but no UTS. (We note that the grafting density for 76S and 209S were only about two-fifths of that for the PNIPAM samples on gold prepared from a solution with a ratio of 90/10 by volume of MU to DT. This indicates that the thiol-SAM packs more densely on gold than does the trichlorosilane initiator on silicon oxide.) The curves through the data correspond to the segment concentration profiles shown in Figure 4b. The segment concentration near the substrate at 20 °C is much lower than that for 76S (not shown), consistent with a much lower grafting density for this sample. Bilayer profiles are again required to fit the data at both 20 and 39 °C. However, the profile at 39 °C is more distinctly bilayer than the corresponding profile in Figure 1b. This was a general trend for the samples synthesized on the two surfaces and suggests that more segmental adsorption occurs for the PNIPAM brushes synthesized on silicon oxide. This conclusion is consistent with a lower packing density for the trichlorosilane initiators on silicon oxide than for the thiol-SAMs on gold. The first moment of the segment concentration profile is plotted as a function of temperature in Figure 5. The first moment of the profile decreased from 693 to 242 Å for 230S. This change is slightly smaller and occurs over a broader temperature range

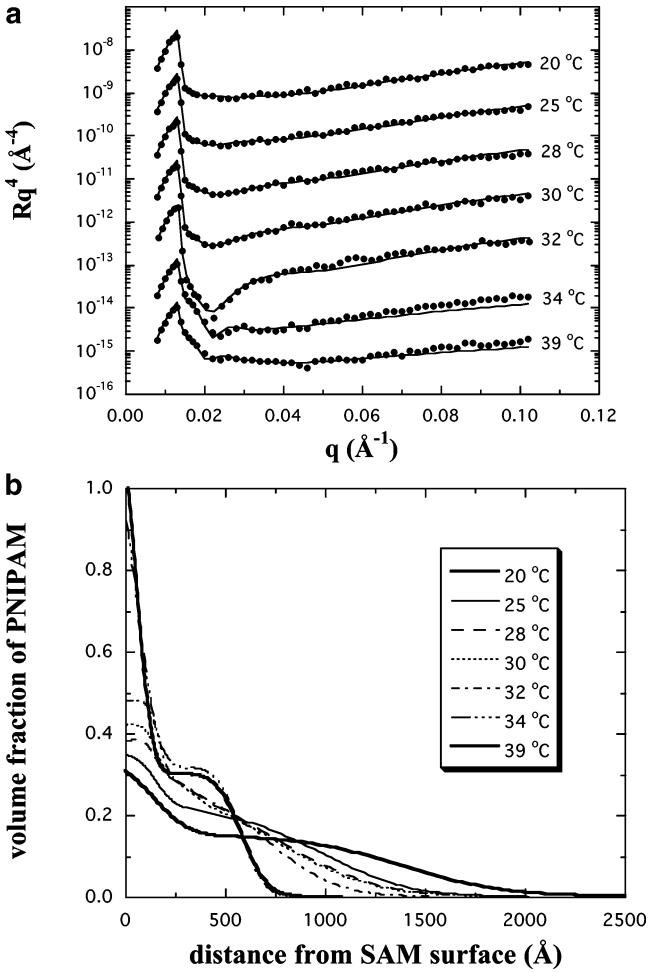

Figure 4. (a) Neutron reflectivity data from 230S for a series of temperatures from 20 °C to 39 °C in D_2O. The curves through the data correspond to the best-fit model segment concentration profiles shown in (b). (b) Best-fit concentration profiles.

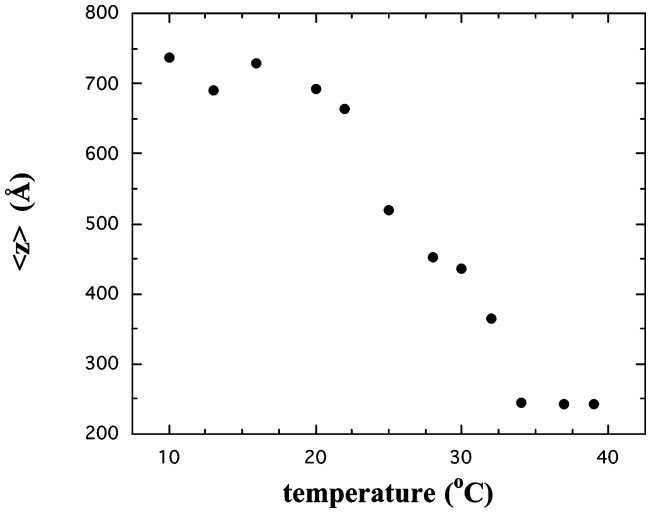

Figure 5. Variation of the first moment of the segment concentration profile with temperature upon heating from 10 to 39 °C for 230S.

than that for 152G, but the change is again much larger than for the samples at higher and lower surface density reported previously.

The relative change of the first moment of the segment concentration profiles at 20 and 40 °C ($\langle z\rangle_{20}/\langle z\rangle_{40}$) for all our samples including those reported previously is plotted as a function of M and σ in Figure 6. The samples synthesized on

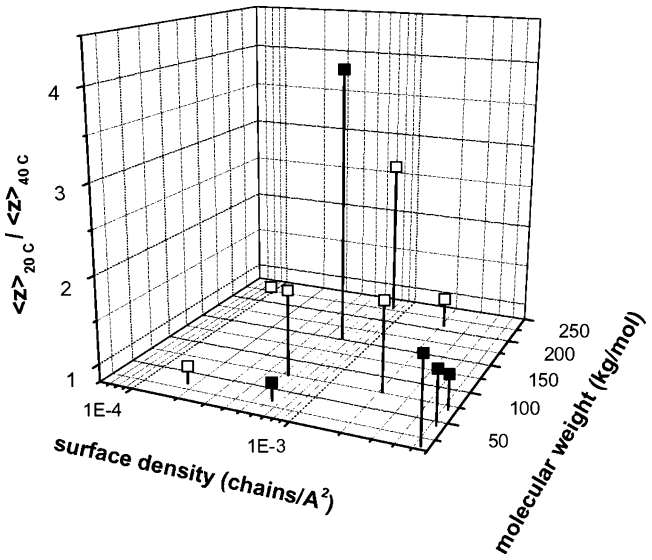

Figure 6. Ratio of the first moment of the segment concentration profile at 20 and 40 °C as a function of molecular weight and surface density. Open (filled) symbols indicate samples grafted from silicon oxide (gold).

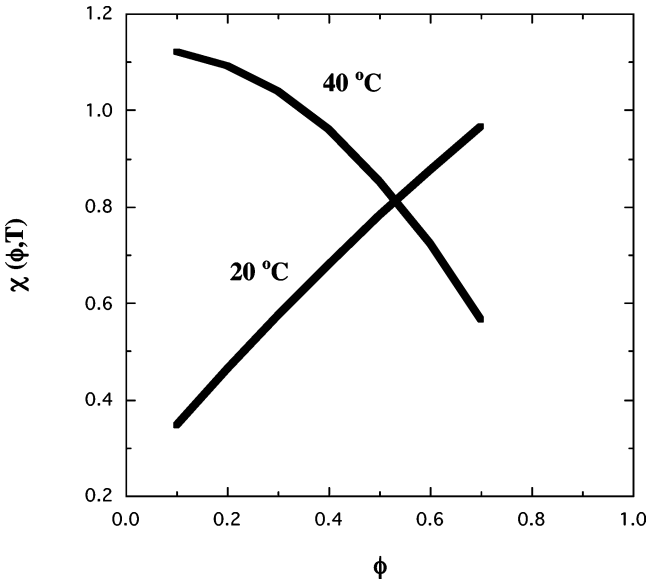

Figure 7. Temperature-dependent effective χ parameter at 20 and 40 °C from the data of Afroze et al.[19]

silicon oxide are denoted by open symbols, and the samples synthesized on gold are denoted by filled symbols. Typical uncertainty in $\langle z \rangle$ is ±15% at 20 °C and ±5% at 40 °C, determined by parameter values that result in an increase in χ^2 by a factor of 1.3. Figure 6 shows that the conformational change of a PNIPAM brush is strongly dependent on the grafting density and molecular weight. PNIPAM brushes with intermediate grafting densities and high molecular weights display the largest conformational change with temperature.

Discussion

The general trends in the data shown in Figure 6 are in good agreement with a numerical SCF calculation reported by Mendez and co-workers.[34] They found that $\langle z \rangle_{20°C}/\langle z \rangle_{40°C}$ contains a maximum at an intermediate value of σ, consistent with our data in Figure 6. They predicted that the maximum in $\langle z \rangle_{20°C}/\langle z \rangle_{40°C}$ increases with M and shifts to lower σ as M increases. Unfortunately, the present data are not sufficient to rigorously test the latter prediction. For a rigorous test, grafted PNIPAM samples with the same molecular weight would need to be prepared over a wide range of grafting density, which is very difficult to do. However, the present data confirm the general trend of a maximum in $\langle z \rangle_{20°C}/\langle z \rangle_{40°C}$ at intermediate coverage and high M. Also, regarding the magnitude of $\langle z \rangle_{20°C}/\langle z \rangle_{40°C}$, they reported values ranging up to 4 for their longest chain length which contained 100 subunits, where a subunit is believed to represent 7−10 monomers. We observed $\langle z \rangle_{20°C}/\langle z \rangle_{40°C} = 4$ for 159S, which has 1350 monomers. A precise comparison is precluded by that fact that the present data are too limited to obtain the maximum $\langle z \rangle_{20°C}/\langle z \rangle_{40°C}$ value as a function of σ for each M. Also, the calculations are inherently 1-D and do not account for in-plane variation in the poor solvent state. Modest variation in in-plane structure with temperature occurs in our samples as measured by AFM.

The general trends of the data in Figure 6 can be simply understood by considering $\chi(\phi)$ along with the well-known chain stretching effect for densely grafted brushes in good solvent conditions. $\chi(\phi)$ obtained from the experimental phase diagram for PNIPAM free chains in water as reported by Afroze and co-workers[19] is plotted in Figure 7. At our highest grafting density, the average ϕ within the layer is large ($\phi = 0.60-0.75$ at the substrate surface for 71G, 44G, and 13G[48]) and from Figure 7 the difference in χ at 20 and 40 °C is relatively small. This explains the weak change in layer thickness with temperature for the PNIPAM samples at our highest grafting densities. As the surface coverage decreases, ϕ within the brush decreases, the solvent quality at 20 °C improves, and the difference in χ at 20 and 40 °C increases. This results in larger values of $\langle z \rangle_{20°C}/\langle z \rangle_{40°C}$ for the high-M samples at intermediate grafting density as seen in Figure 6. The strong dependence of the conformational change on M at intermediate σ is due to the chain stretching effect previously studied in detail in UCST systems.[14−18] The amount of chain stretching has been shown empirically to be determined largely by the value of $\Sigma = \sigma\pi R_g^2$.[18] For fixed σ, Σ increases with increasing M, leading to increased chain stretching in good solvent conditions. Thus, the maximum in $\langle z \rangle_{20°C}/\langle z \rangle_{40°C}$ at intermediate σ appears to arise from a competition between the chain stretching effect which increases with σ and M and the fact that the temperature dependence of $\chi(\phi)$ becomes weak at high σ. We note that a maximum in $\langle z \rangle_{\text{good solvent}}/\langle z \rangle_{\text{poor solvent}}$ should also occur as a function of σ for UCST systems because the conformational change with temperature or solvent quality will become weak at very high grafting density where the chains are close packed and have little room to collpase. However, in that case the maximum should be much weaker and occur at higher σ.

At 40 °C and $\phi < 0.7$, the tethered system has passed well into the two-phase coexistence regime for free PNIPAM chains, and correspondingly the grafted chains have collapsed onto the surface. For this reason the conformational change in the PNIPAM system is much more pronounced than for a typical UCST system over the same range of temperature.

In Figure 6, the PNIPAM layers at the lowest σ show very little change with temperature. The surface density ranged from 1×10^{-4} to 2×10^{-4} chains/Å^2, and Σ ranged from 2 to 9 for these samples, assuming no segmental adsorption. The experimental profiles reported previously[44] indeed suggested strong segmental adsorption, and in that case Σ of the dangling chains would have been lower than the above estimate. The low values of Σ explain the lack of conformational change with T for these low σ samples. For sufficiently low σ, the calculations of Mendez et al. show a very weak and almost linear decrease in $\langle z \rangle$ over a wide range of T (from 10 to 50 °C).

While there is good qualitative agreement between our results and the calculations of Mendez et al. with respect to the general trend described above, some discrepancies exist. Mendez et al. calculated the shift in the two-phase coexistence curve that results from the tethering constraint. Their calculations predict that coexistence occurs at lower T for higher σ and that the difference in the composition of the two coexisting phases is greater with increasing σ. Thus, for tethered PNIPAM chains at low to intermediate σ, they predict that the transition shifts to lower T with increasing σ and becomes more pronounced. The magnitude of the predicted shift is about 14 °C for an increase in σ of a factor of 3. Figure 2 shows that for 152G the transition is well-defined and occurs at 29 °C. For 230S, which has slightly higher surface density, the transition occurs at 27.5 °C. While the trend for these samples with intermediate surface density and high M is consistent with the prediction, at high surface density and high M an entirely different phenomenon occurs. As reported elsewhere,[61] at high surface density and high M the change in profile shape through the transition is nonmonotonic. The form of the $\langle z \rangle$ vs T plots is significantly altered, and in the most extreme cases (71G and 209S) a maximum in $\langle z \rangle$ as a function of T occurs near 30 °C. We believe this to be due to vertical phase transition within the brush,[32,33] which is not predicted in the calculations of Mendez et al.

Another discrepancy is that the trend with M seen for 13G, 44G, and 71G at the highest grafting density on gold in Figure 6 does not follow the predictions of Mendez et al. The same trend holds for the samples with the highest grafting density on silicon oxide, 76S and 209S. In particular, the values of $\langle z \rangle_{20°C}/\langle z \rangle_{40°C}$ at lower M in each series are larger than expected in comparison with the other data. Elsewhere, we reported that the higher values of $\langle z \rangle_{20}/\langle z \rangle_{40}$ at lower M for the samples on gold correlated with increased bilayer character in the profiles at 20 °C.[48] The same result holds for 76S and 209S, although 209S also has substantial bilayer character, much more than 71G. We previously argued this may be due to lateral heterogeneity within the low M brushes at high σ.[48] However, the higher $\langle z \rangle_{20}$ and the increasing bilayer character of the 20 °C profiles with decreasing M for the high σ samples can also be explained by vertical phase separation within the brush, if it occurs at lower T for lower M. As mentioned above, we previously reported that the first moment of the profile increases when vertical phase separation occurs.[61] Thus, vertical phase separation would be consistent with the anomalously high first moment as well as the increased bilayer character of the profiles at 20 °C for the lower M samples at high σ. However, we do not understand why vertical phase separation results in an increase in the first moment nor do we understand why this phenomenon would occur at lower T for lower M.

Conclusions

Some applications of grafted PNIPAM layers will depend critically on the magnitude of chain conformational changes. Therefore, it is important to understand how to manipulate the conformational change to optimize the system for specific applications. Neutron reflectivity was applied to study the temperature-dependent conformational change of PNIPAM chains grafted over a range of surface density and molecular weight. Samples were synthesized on silicon oxide and also on gold. Our study shows that the conformational change of the grafted PNIPAM brushes varies greatly with molecular weight and grafting density. The maximum conformational change was observed for PNIPAM brushes with high molecular weight and intermediate grafting density. This trend is in good agreement with a self-consistent-field calculation of Mendez and co-workers. Thus, this study provides new insight that can be used to optimize PNIPAM brushes for applications that require large conformational changes.

Acknowledgment. Sandia is a multiprogram laboratory operated by Sandia Corporation, a Lockheed Martin Company, for the United States Department of Energy under Contract DE-AC04-94AL85000. We acknowledge the support of the National Institute of Standards and Technology, U.S. Department of Commerce, in providing the neutron research facilities used in this work and also support from the Office of Naval Research.

References and Notes

(1) Lin, S.-Y.; Chen, K.-S.; Chu, L.-R. *Polymer* **1999**, *40*, 2619.
(2) Katsumoto, Y.; Tanaka, T.; Sato, H.; Ozaki, Y. *J. Phys. Chem. A* **2002**, *106*, 3429.
(3) Percot, A.; Zhu, X. X.; Lafleur, M. *J. Polym. Sci., Polym. Phys.* **2000**, *38*, 907.
(4) Schild, H. G. *Prog. Polym. Sci.* **1992**, *17*, 163.
(5) Hoffman, A. S. *J. Controlled Release* **1987**, *6*, 297.
(6) Stayton, P. S.; Shimoboji, T.; Long, C.; Chilkoti, A.; Chen, G.; Harris, J. M.; Hoffman, A. S. *Nature (London)* **1995**, *378*, 472.
(7) Feil, H.; Bae, Y. H.; Jan, F.; Kim, S. W. *J. Membr. Sci.* **1991**, *64*, 283.
(8) Park, Y. S.; Ito, Y.; Imanishi, Y. *Langmuir* **1998**, *14*, 910.
(9) Yamada, N.; Okano, T.; Sakai, H.; Karikusa, F.; Sawasaki, Y.; Sakurai, Y. *Makromol. Chem., Rapid Commun.* **1990**, *11*, 571.
(10) Okano, T.; Yamada, N.; Okuhara, M.; Sakai, H.; Sakurai, Y. *Biomaterials* **1995**, *16*, 297.
(11) Kawaguchi, H.; Fujimoto, K.; Mizuhara, Y. *Colloid Polym. Sci.* **1992**, *270*, 53.
(12) Okano, T.; Kikuchi, A.; Sakurai, Y.; Takei, Y.; Ogata, N. *J. Controlled Release* **1995**, *36*, 125.
(13) Ista, L. K.; Perez-Luna, V. H.; Lopez, G. P. *Appl. Environ. Microbiol.* **1999**, *65*, 2552.
(14) Milner, S. T. *Science* **1991**, *251*, 905.
(15) Halperin, A.; Tirrell, M.; Lodge, T. P. *Adv. Polym. Sci.* **1992**, *100*, 31.
(16) Szleifer, I.; Carignano, M. A. *Adv. Chem. Phys.* **1996**, *94*, 165.
(17) Grest, G.; Murat, M. *Monte Carlo and Molecular Dynamics Simulations in Polymer Science*; Binder, K. Ed.; Clarendon Press: Oxford, 1994.
(18) Kent, M. S. *Macromol. Rapid Commun.* **2000**, *21*, 243 and references therein.
(19) Afroze, F.; Nies, E.; Berghmans, H. *J. Mol. Struct.* **2000**, *554*, 55.
(20) Matsuyama, A.; Tanaka, F. *Phys. Rev. Lett.* **1990**, *65*, 341.
(21) Bekiranov, S.; Bruinsma, R.; Pincus, P. *Phys. Rev. E* **1997**, *55*, 577.
(22) Dormidontova, E. *Macromolecules* **2002**, *35*, 987.
(23) Karlstrom, G. *J. Phys. Chem.* **1985**, *89*, 4962.
(24) de Gennes, P.-G. *C. R. Acad. Sci. Paris II* **1991**, *117*, 313.
(25) Bjorling, M.; Linse, P.; Karlstrom, G. *J. Phys. Chem.* **1990**, *94*, 471.
(26) Wagner, M.; Brochard-Wyart, F.; Hervet, H.; de Gennes, P.-G. *Colloid Polym. Sci.* **1993**, *271*, 621.
(27) Linse, P. *Macromolecules* **1994**, *27*, 6404.
(28) Bjorling, M. *Macromolecules* **1992**, *25*, 3956.
(29) Svensson, M.; Alexandritis, P.; Linse, P. *Macromolecules* **1999**, *32*, 637.
(30) Halperin, A. *Eur. Phys. J. B* **1998**, *3*, 359.
(31) Sevick, E. M. *Macromolecules* **1998**, *31*, 3361.
(32) Baulin, V. A.; Halperin, A. *Macromol. Theory Simul.* **2003**, *12*, 549.
(33) Baulin, V. A.; Zhulina, E. B.; Halperin, A. *J. Chem. Phys.* **2003**, *119*, 10977.
(34) Mendez, S.; Curro, J. G.; McCoy, J. D.; Lopez, G. P. *Macromolecules* **2005**, *38*, 174.
(35) Mattice, W. L.; Misra, S.; Napper, D. H. *Eurphys. Lett.* **1994**, *28*, 603.
(36) Balamurugan, S.; Mendez, S.; Balamurugan, S. S.; O'Brien, M. J., II; Lopez, G. P. *Langmuir* **2003**, *19*, 2545.
(37) Kidoaki, S.; Ohya, S.; Nakayama, Y.; Matsuda, T. *Langmuir* **2001**, *17*, 2402.
(38) Jones, D. M.; Smith, J. R.: Huck, W. T. S.; Alexander, C. *Adv. Mater.* **2002**, *14*, 1130.
(39) Walldal, C.; Wall, S. *Colloid Polym. Sci.* **2000**, *278*, 936.
(40) Zhu, P. W.; Napper, D. H. *J. Colloid Interface Sci.* **1994**, *164*, 489.
(41) Zhu, P. W.; Napper, D. H. *Colloids Surf. A* **1996**, *113*, 145.
(42) Wu, T.; Efimenko, K.; Vlcek, P.; Subr. V.; Genzer, J. *Macromolecules* **2003**, *36*, 2448.
(43) Hu, T.; Wu, C. *Phys. Rev. Lett.* **1999**, *83*, 4105.

(44) Yim, H.; Kent, M. S.; Huber, D. L.; Satija, S.; Majewski, J.; Smith, G. S. *Macromolecules* **2003**, *36*, 5244.
(45) Okahata, Y.; Noguchi, H.; Seki, T. *Macromolecules* **1986**, *19*, 494.
(46) Stayton, P. S.; Shimoboji, T.; Long, C.; Chilkoti, A.; Chen, G.; Harris, J. M.; Hoffman, A. S. *Nature (London)* **1995**, *378*, 472.
(47) Yim, H.; Kent, M. S.; Mendez, S.; Balamurugan, S. S.; Balamurugan, S.; Lopz, G. P.; Satija, S. *Macromolecules* **2004**, *37*, 1994.
(48) Yim, H.; Kent, M. S.; Satija, S.; Mendez, S.; Balamurugan, S. S.; Balamurugan, S.; Lopz, G. P. *J. Polym. Sci., Part B: Polym. Phys.* **2004**, *42*, 3302.
(49) In refs 47 and 48, we reported a surface density of 3.1×10^{-3} chains/Å^2 for 71G. This value was obtained assuming that the melt density of PNIPAM is 1 g/cm^3. However, the density obtained from the measured SLD of the dry sample is 1.76 g/cm^3, which corresponds to the value 5.4×10^{-3} chains/Å^2 reported above.
(50) Certain trade names and company products are identified in order to specify adequately the experimental procedure. In no case does such identification imply recommendation or endorsement by the National Institute of Standards and Technology, nor does it imply that the products are necessarily the best for the purpose.
(51) Matyjaszewski, K.; Miller, P. J.; Shukla, N.; Immaraporn, B.; Gelman, A.; LuoKala, B. B.; Siclovan, T. M.; Kickelbick, G.; Vallant, T.; Hoffmann, H.; Pakula, T. *Macromolecules* **1999**, *32*, 8716.
(52) Kaholek, M.; Lee, W.-K.; Ahn, S.-J.; Ma, H.; Caster, K. C.; LaMattina, B.; Zauscher, S. *Chem. Mater.* **2004**, *16*, 3688.
(53) Varshney, S. (Polymer Source), personal communication.
(54) Ejaz, M.; Tsuji, Y.; Fukuda, T. *Polymer* **2001**, *42*, 6811.
(55) Deveau, C.; Chapel, J. P.; Boyou, E.; Chaumont, Ph. *Eur. Phys. J. E* **2002**, *7*, 345.
(56) Kizhakkedathu, J. N.; Norris-Jones, R.; Brooks, D. E. *Macromolecules* **2004**, *37*, 734.
(57) In ref 42, a difference of 3−5 was reported in a similar comparison between molecular weights for surface polymerized and solution polymerized samples. This substantial discrepancy between the results in ref 42 and the results in refs 54−56 may possibly be due to the very small pores of the supporting matrix in ref 42.
(58) Styrkas, D.; Doran, S. J.; Gilchrist, V.; Keddie, J. L.; Lu, J. R.; Murphy, E.; Sackin, R.; Su, T.-J.; Tzitzinou, A. *Polymer Surfaces and Interfaces III*; Richards, R. W., Peace, S. K., Eds.; John Wiley & Sons Ltd.: New York, 1999.
(59) Russell, T. P. *Mater. Sci. Rep.* **1990**, *5*, 171.
(60) Yim, H.; Kent, M. S.; Hall, J. S.; Benkoski, J. J.; Kramer, E. J. *J. Phys. Chem. B* **2002**, *106*, 2474.
(61) Yim, H.; Kent, M. S.; Satija, S.; Mendez, S.; Balamurugan, S. S.; Balamurugan, S.; Lopz, G. P. *Phys. Rev. E* **2005**, *72*, 051801.
(62) Baulin, V. A.; Zhulina, E. B.; Halperin, A. *J. Chem. Phys.* **2003**, *119*, 10977.
(63) Baulin, V. A.; Halperin, A. *Macromol. Theory Simul.* **2003**, *12*, 549.

MA0520949